Simulations and potentiometric titrations enable reliable determination of effective pKa values of various polyzwitterions

Raju Lunkad,[1,a] Philip Biehl,[2,3,4,a] Anastasiia Murmiliuk,[5] Pablo M. Blanco,[1,6] Peter Mons,[2,3,4] Miroslav Štěpánek,[1] Felix Schacher,[2,3,4,*] Peter Košovan[1*]

[1]*Department of Physical and Macromolecular Chemistry, Faculty of Science, Charles University, Hlavova 8, 128 40 Prague 2, Czech Republic*
[2]*Institute of Organic Chemistry and Macromolecular Chemistry (IOMC), Friedrich-Schiller-University Jena, Lessingstraße 8, D-07743 Jena, Germany*
[3]*Jena Center for Soft Matter (JCSM), Friedrich-Schiller-University Jena, Philosophenweg 7, D-07743 Jena, Germany*
[4]*Center for Energy and Environmental Chemistry (CEEC), Friedrich-Schiller-University Jena, Philosophenweg 7, D-07743 Jena, Germany*
[5]*Jülich Centre for Neutron Science JCNS at Heinz Maier-Leibnitz Zentrum (MLZ), Forschungszentrum Jülich GmbH, Lichtenbergstraße 1, 85748 Garching, Germany*
[6]*Department of Material Science and Physical Chemistry, Research Institute of Theoretical and Computational Chemistry (IQTCUB), University of Barcelona, C/Martí i Franquès 1, 08028 Barcelona, Spain*

(a) The two authors contributed equally

* corresponding authors peter.kosovan@natur.cuni.cz felix.schacher@uni-jena.de

TOC graphic “for Table of Contents use only”

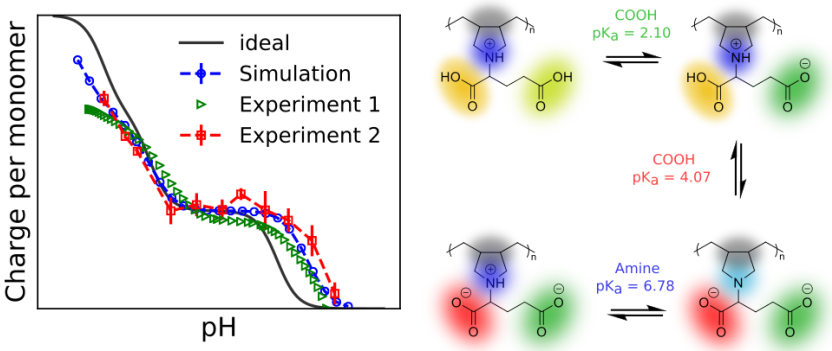

Abstract

We synthesized three different polyzwitterions: poly(*N,N*-diallylglutamate) (PDAGA), polydehydroalanine (PDha), poly(2-(imidazol-1-yl)acrylic acid) (PImAA), and investigated how their ionization states respond to changes in solution pH. We used molecular simulations to determine how the net charge per monomer and the ionization states of individual acidic and basic groups differ from the ideal (Henderson-Hasselbalch) behavior. To complement the theoretical predictions, we performed potentiometric titrations and zeta potential measurements of all studied polyzwitterions. By comparing these experiments with theoretical predictions we could show that molecular simulations can predict and explain the origin of the differences between the effective and bare pK_a values of individual titratable groups. Furthermore, we have shown that it is not possible to obtain these effective pK_a values directly from the equivalence point recognition criterion (ERC), commonly used in potentiometric titrations. However, the effective pK_a values can be reliably obtained by calculating the net charge per monomer from the potentiometric titration curves and validating these results against theoretical predictions. The approach we propose works reliably for polyzwitterions in which the ionization response is dominated by electrostatic interactions, such as PDAGA or PDha, however, it fails if other specific interactions contribute significantly, such as in the case of PImAA.

Introduction

Polyzwitterions represent an outstanding class of polymers that are currently discussed as potential third generation of antifouling materials to overcome issues and expand the application field of conventional antifouling materials like poly(hydroxyethyl methacrylate) (PHEMA) or poly(ethyleneglycol) (PEG) based systems.[1] The constant interest in these materials is mainly based on their exceptional solution properties which feature high hydrophilicity, solution stability under saline conditions, and responsive behavior towards temperature and/or pH.[2] These properties arise from the interplay of charged functional groups along the polymer to one another and towards their surroundings. Unlike typical polyelectrolytes, with either poly-cationic or -anionic structure, polyzwitterions express both anionic and cationic functionalities on the same pendant groups.[3] This balanced charge of ionized groups can yield a zero net charge while at the same time allowing strong electrostatically induced hydration of the material due to strong dipole pairs, rendering the polymers with a tightly bound hydration layer and thus reduced bimolecular interactions.[2]

Since zwitterionic structures occur in many biological structures like phosphatidylcholine in cell membranes, amino acids, or betainic structures it is not surprising that artificial materials mimicking these structures typically exhibit good biocompatibility,[4] cell and protein repellence ,[5] non-thrombogenic properties, and hemocompatibility.[6] In contrast to common hydrophilic polymer systems, which tend to collapse upon the addition of salt, polyzwitterions tend to stretch and maintain their hydrophilicity under such conditions.[7] This provides exceptional stability for the application in fields like marine surfaces[8] or as a coating for the stabilization of dispersed materials in biological fluids.[9] Furthermore, the observed immune response of patients (approximately 20% of healthy human subjects) towards PEGylated systems is a strong driving force to generate alternative systems with comparable stealth effects while simultaneously avoiding the polyether structure.[10] With these exciting properties, polyzwitterions are not only of academic interest but they also find applications in commercial products, ranging from surface coatings for hip-replacements (Kyocera, Aquala®) and Implantable ventricular assist devices (EVAHEART®), to zwitterionic membranes for industrial wastewater treatment (ZwitterCo, Inc.).

Because most of the interesting properties of polyzwitterions are based on the charged moieties, the overall charge distribution and charge density of these systems become an important parameter of their design. Key questions for further successful implementation of polyzwitterions in the biomedical field lie in the area of interface research, where surface immobilization techniques,[11] but also the interactions of polyzwitterions with their environment (cell adhesion, protein corona formation) are in the focus of current discussions.[12] The majority of polyzwitterions synthesized today carry permanently charged groups, such as quaternary amines or strong acids, which ensures that their net charge is not affected by a change in the pH.[13] However, the response to pH can be beneficial for biomedical applications. The variation of pH, observed in inflammatory or cancerogenic tissue,[14] can be used to trigger the release or accumulation response of nanocarriers based

on polyampholytes.[15] In contrast to the most common polyzwitterions, examples featuring weak ionizable groups allow a variation of the charge along the polymer upon a change in pH.[16] These polymers can be described as annealed polyampholytes[17] or weak polyzwitterions and open up a way for pH responsive materials and surfaces.[18]

We showed earlier[19] that polydehydroalanine (PDha), as an example of a weak polyzwitterion, is a unique and highly interesting polymer in terms of charge density and its ability to fully invert charge upon variation of the pH value. The application of this polymer as a coating material for nanocarriers[20] made use of its charge inversion for the adsorption and the release of charged dye molecules,[21] polyelectrolytes, and proteins[22] and with that is of interest for triggered release of molecules on the nanoscale. Besides PDha we investigated further weak polyzwitterions such as (poly(2-(imidazole-1-yl)acrylic acid) (PImAA) and poly(*N,N*-diallylglutamate) (PDAGA) as coating materials for nanoparticles to generate a small platform of nanocarriers with an individual pH response depending on the respective coating material.[22] Despite the marked success in the use of weak polyampholytes as smart pH-responsive materials, further progress in this field requires a deeper understanding of the mechanisms controlling their pH-dependent charge, which in turn determines their solution properties.

The Henderson-Hasselbalch equation serves as a starting point for the theoretical description, since it allows to calculate the ionization degree of ionisable group from the pH and its intrinsic pK_a value as

$$\alpha^{ID} = \frac{1}{1+10^{z\,(pH-pK_{a,i})}} \qquad (1)$$

where z_i is the charge of the group *i* in the ionized state. In principle the Henderson-Hasselbalch equation ultimately allows calculating the net charge per monomer on the polymer consisting of multiple titratable groups. However, such an approach can be

considered only as a null model because it completely neglects interactions between the charged groups. Furthermore, interactions between different groups on a polyelectrolyte chain often significantly affect its conformation, which in turn affects the interactions, creating a complicated feedback mechanism. This feedback mechanism is difficult to describe by an analytical theory, however, it can be described in molecular simulations.

In a molecular simulation, we start by defining the model which we use to represent the studied molecules. Then, we generate a set of conformations of the studied molecules in various ionization states and compute the macroscopic properties of the molecules as an average over the ensemble of the generated configurations. Simulation models with all-atom resolution often require a prohibitive amount of computational resources when used to study polymers in solution. Therefore, it is desirable to use simplified models which abandon some molecular details while accounting for the most important effects. Then, the simulation results can be used to explain the macroscopic properties on the molecular level. Specifically, when studying acid-base equilibria, the simulations predict the net charge on the macromolecule as well as the degree of ionization of individual acid and base groups at a particular value of the pH. They can also predict how this ionization is affected by electrostatic interactions and by the conformations of the simulated macromolecules. However, it is not known *a priori* to what extent the simplifications introduced in the model affect the predicted properties. Therefore, the simulation predictions should always be confronted with an independent experimental characterization.

Experimental determination of net charge on a polyelectrolyte or its degree of ionization is a challenging task. Among the established analytical methods, there is none that would yield the net charge as its direct output. Usually, the net charge is inferred indirectly, from quantities such as the zeta potential or electrophoretic mobility.[23–27] However, there is no simple relation between the directly measured quantities and the net charge, which is the

ultimate quantity of interest. Alternatively, one can determine the degree of ionization from the changing positions or intensities of specific peaks in the NMR or infra-red spectra.[26–29] However, these peaks may be affected by other processes, not only the ionization states, and it may be difficult to disentangle various contributing effects. Another alternative to determine the charge or ionization states of polyelectrolytes is based on potentiometric titrations. When studying small molecules, the equivalence point in the titration indicates when an acid or base group has been fully neutralized by the titrant. The maximum in the first derivative of the titration curve, i.e. dependence of the pH on the added volume of the titrant, is usually used as the equivalence point recognition criterion (ERC). The effective pK_a of that group, i.e. the pH at which the group is half-ionized, is then determined from the half-equivalence point, i.e. the pH corresponding to one half of the added volume of the titrant required to reach the equivalence point.[30] In the case of multiprotic acids or bases, additional pKa values can be found half-way between two consecutive equivalence points.[31–34] In the case of a polyelectrolyte, the pH at which a given acid or base group is half-ionized, determines the effective pKa of that group. This effective pKa of a polyelectrolyte often significantly differs from the bare pKa of the corresponding monomer. However, as follows from our current work, often the above-mentioned ERC is not a good indicator of this effective pKa. Nevertheless, it is possible to calculate the net charge on the macromolecule directly from the potentiometric titration curves. Such a calculation can be precise only if various artifacts, such as the presence of additional ions in the solution or the adsorption of CO_2 from the air are carefully avoided.[27,35–37] In either case, the experimental determination of net charge or ionization states of titratable groups is based on various assumptions that need not be fulfilled. Therefore, if one wants to reliably determine the charge on a complex polymeric species, it is necessary to use several independent experimental methods. These should be then compared with each other, as well as with the predictions from theory or simulations.

In this work, our aim is to better understand net charge and charge distribution within different weak polyampholytes, materials we have introduced earlier and which show very interesting material properties. More specifically, we are interested in a comprehensive understanding of the pH-controlled ionization of PDAGA, PDha and PImAA. These polymers possess the interesting ability to switch their net charge from positive to negative upon a change in pH. In all three cases, the titratable weak acid and base groups responsible for this switching behavior are carboxylic acids and amines, as is schematically illustrated in Fig.1. However, these groups have different individual pK_a values and also the amount of the titratable groups per monomeric unit is different too: one carboxylic group and one primary amine group in PDha; two carboxylic groups and one tertiary amine in PDAGA; one carboxylic group and one imidazole group in PImAA. Therefore, these two polymers follow different trends of the net charge as a function of pH, resulting in an overall different solution behavior. To understand how their variable ionization depends on the pH, we combine theoretical predictions from computer simulations with several independent experimental methods that allow determining their net charge or ionization states.

Materials and methods

Materials

Chemicals were purchased from Sigma–Aldrich or Carbolution (Saarbrücken, Germany) in p.a. grade and used without further purification. The UV photoinitiator, Lucirin-TPO ((diphenylphosphoryl) (mesityl)methanone), was kindly provided by BASF. All chemicals were used as received.

Synthesis of Poly(N,N-diallylglutamate) (PDAGA)

The synthesis of PDAGA was originally reported by Jamiu *et al.*[38] HCl was introduced to a suspension with 59 g of glutamic acid (0.4 mol) in 500 mL of methanol at 0°C. Then, the

solution was stirred for 3 days. After removing the solvent, the obtained product was dissolved in 100 mL of water and neutralized with K_2CO_3 at 0°C. Next, the mixture was saturated with K_2CO_3 and extracted 5 times with 100 mL of $CHCl_3$. After drying, the residual product (61 g, 87%) was dissolved in a solution of 87 g K_2CO_3 (0.63 mol) in 300 mL of acetonitrile at 40–50 °C. Then, 85g of allyl bromide (0.70 mol) was added dropwise. The mixture was stirred at 60 °C for 18 h. After removing the solvent, the residue was picked up in 200 mL of water and extracted 3 times with 100 mL of ether. The organic layer was dried, concentrated, and distilled to obtain the corresponding diallylamine derivative as a colorless liquid. 5.4 g of this liquid was treated with 2 g of NaOH in 15 mL water. After one day, the solution was adjusted to a pH = 3 with HCl. The viscous solution was freeze-dried. The obtained solid was extracted with 30 mL acetone at 60°C. After evaporation of acetone, the monomer was obtained as white flakes. The following cyclopolymerization was carried out by dissolving 1.44 g of the monomer in 0.5 mL water. The solution was degassed and heated to 85°C. 133 µg of APS was added to the solution while stirring it and left it to rest for 15 min. Subsequently the mixture was cooled to room temperature and the polymer was obtained by dialyzing the mixture against water for 3 days. Finally, once the mixture was freeze-dried, a white powder was obtained.

Synthesis of Polydehydroalanine (PDha)

PDha was prepared as reported by Günther *et al.*[19]. 250 mg of poly(aminomethyl acrylate) (PAMA) was dissolved in 10 mL of 1,4-dioxane. Then, 10 mL of a saturated solution of LiOH was added. The mixture was stirred at 100 °C for 3 h and neutralized with a diluted aqueous solution of HCl. During neutralization, PDha precipitated.

Synthesis of Poly(2-(imidazol-1-yl)acrylic Acid) (PImAA)

PImAA was synthesized as reported by Rössel *et al.*[39] . Briefly, DMSO (1.75 M EImA) and AIBN (0.5 mol %) were added to a flask charged with ethyl 2-(imidazol-1-yl)acrylate (EImA).

The mixture was degassed by three freeze–pump–thaw cycles and held at 65 °C for 48 h. The resulting polymer was precipitated afterward in EtOAc (45 mL), centrifuged, and dried under vacuum. The obtained PEImA (101.7 mg) was dissolved in methanol (2 mL), and a solution of lithium hydroxide monohydrate (162.3 mg, 3.87 mmol, 5 equiv per monomer unit) in water (2 mL) was added. The reaction mixture was held at 65 °C for 48 h and dialyzed against water. The aqueous solution of the polymer was freeze-dried and afforded 75.7 mg of PImAA as a white solid.

Nuclear magnetic resonance spectroscopy (NMR)

^{1}H-NMR spectra were measured on a 300 MHz Bruker AVANCE spectrometer using D_2O with NaOD as deuterated solvents at a temperature of 298 K. The solvent residual peak of the respective solvent was used as standard.

Size exclusion chromatography (SEC)

SEC measurements were performed on a Agilent system equipped with a G1310A pump, and a RID: G7162A refractive index detector with DMAc + 0.21 wt.% LiCl as eluent at a flow rate of 1 mL min^{-1} on a PSS GRAM guard/30/1,000 Å (10 µm particle size) column at 40°C.

Aqueous SEC was measured on a Jasco system equipped with a DG-2080-53 degasser, PU-980 pump, and a RI-2031 Plus refractive index detector (Jasco Deutschland Labor- und Datentechnik GmbH, Groß-Umstadt, Germany) with 0.1 m Na_2HPO_4/0.05% NaN_3 pH = 9 as eluent and at a flow rate of 1 mL min^{-1} on a column set of PSS SUPREMA 1000 Å and 30 Å (10 µm) at 30°C (PSS, Mainz, Germany). PAA was used as calibration.

Potentiometric titrations

The potentiometric titrations of PDAGA and PImAA were carried out on an OMNIS Advanced Titrator (Deutsche METROHM Prozessanalytik GmbH & Co. KG, Filderstadt, Germany) equipped with a magnetic stirrer, a Pt1000 temperature sensor, and an intelligent

dosing module. For pH detection, either an ECOTRODE plus pH-glass electrode, or a BIOTRODE was used. The polyzwitterions were dissolved in basic Milli-Q water (adjusted by 0.1 M NaOH) resulting in a 0.2 mg mL^{-1} solution with a pH between 10 and 12 and subsequently titrated with 0.1 M HCl at a dosing rate of 0.01 mL min^{-1}. For zeta potential measurements, the titration was paused at the desired pH value and then continued.

The potentiometric titration for PDhA polymer was performed using Metrohm 888 Titrando Compact titrator equipped with a Metrohm LL Biotrode 3 mm glass electrode, a Pt1000 temperature sensor, magnetic stirrer and Titrando Software. Standardised HCl and NaOH solutions from Carl Roth GmbH (Karslruhe, Germany) used for sample preparation and titration were kept under soda lime for at least 2 days before the measurements to prevent CO2 absorption. PDhA was dissolved in 0.1 M NaOH to adjust polymer concentration 10 mg mL^{-1} and titrated by 0.1 M HCl.

We calculated the charge per monomer from our potentiometric titration using the known volumes of HCl and NaOH, as described in Ref.[27]

$$z_m = \frac{V_{HCl}c_{HCl} - V_{NaOH}c_{NaOH} + (c_{OH} - c_H)(V_{HCl} + V_{NaOH})}{c_m V_{NaOH}} \quad (2)$$

where V_x and c_x are the volume and concentration of x = HCl, NaOH and c_m is the concentration of monomeric units of the polyzwitterion.

Zeta potential measurements

The zeta potentials were measured on a Zeta Sizer Nano ZS from Malvern via the M3-PALS technique with a laser beam at 633 nm. The detection angle was 13°.

Theoretical model

We used a coarse grained model to represent the polyzwitterions, where each monomeric unit was represented by two or three spherical beads, as is schematically illustrated in Fig.1.

For brevity, we provide here a brief description of the model and refer the reader to the supporting information (SI) for full technical details. We represented each monomeric unit by one bead for the backbone and one side-bead per each ionisable group. All beads had the same size (σ = 0.35 nm) and they are distinguished only by their acid-base properties, defined by its intrinsic pK_a value, protonation state, and their respective charge. The beads were neutral in the non-ionised state and they carry an elementary charge in the ionized state (±1e for acid or base, respectively). We neglected other specific molecular interactions in our model. This is a reasonable approximation, as long as electrostatic interactions dominante the molecular interactions influencing the ionization states.[40,41] *A posteriori*, we verified the validity of this assumption by comparing with experimental measurements. Similar coarse-grained models are common in polymer science and have been used in our previous publications to model polyelectrolytes,[42–46] short peptides[26,27,41] and disordered proteins.[47]

The intrinsic pK_a values of each acidic and basic group on the monomeric units of the polyzwitterions are the key input parameter of our simulations. We estimated the intrinsic pK_a values using the reported pKa values of the parent monomers of the polyzwitterions, reported in the literature. Specifically, we used the pK_a values of glutamic acid for PDAGA[48] and pK_a values of alanine for PDha.[49] Unfortunately, the intrinsic pK_a values of imidazoleacetic acid, which is the parent monomer of PImAA, are not available from experiments. Therefore, we estimated them using the theoretical prediction provided by the Human Metabolome Database.[50] We emphasize that these pK_a values should be viewed as reasonable estimates, yet not as accurate values.

We simulate the system using molecular simulations which combine Langevin Dynamics accounting for the evolution of configurations and a constant-pH Monte Carlo algorithm accounting for the acid-base equilibrium of all ionisable groups. The simulations included one polyzwitterion chain of 10 monomers accompanied by monovalent salt ions. We tested

that our simulations do not have any significant size effects from the chain length of the polyzwitterion (See SI). We fix the volume of our simulation box to match the concentration of monomeric units used in the titration experiments: 0.022 M (PDAGA), 0.057 M (PDha) and 0.057 M (PImAA). Accordingly, we place the number of ions in the simulations to match the ionic strength of 0.1 M used in the same experiments. Input parameters are the pK_a-values of each ionisable group and the pH of the solution. In return, we measure the average degree of ionization α of each group, which we use to calculate the average charge per monomer z_m as

$$z_m = \sum_{i=1}^{M} z_i \alpha_i \qquad (3)$$

where *M* is the number of ionizable groups in the monomer and z_i is the charge of the group *i* in the ionized state; *i.e.* $z_i = -1$ for a monoprotic acid and $z_i = +1$ for a base.

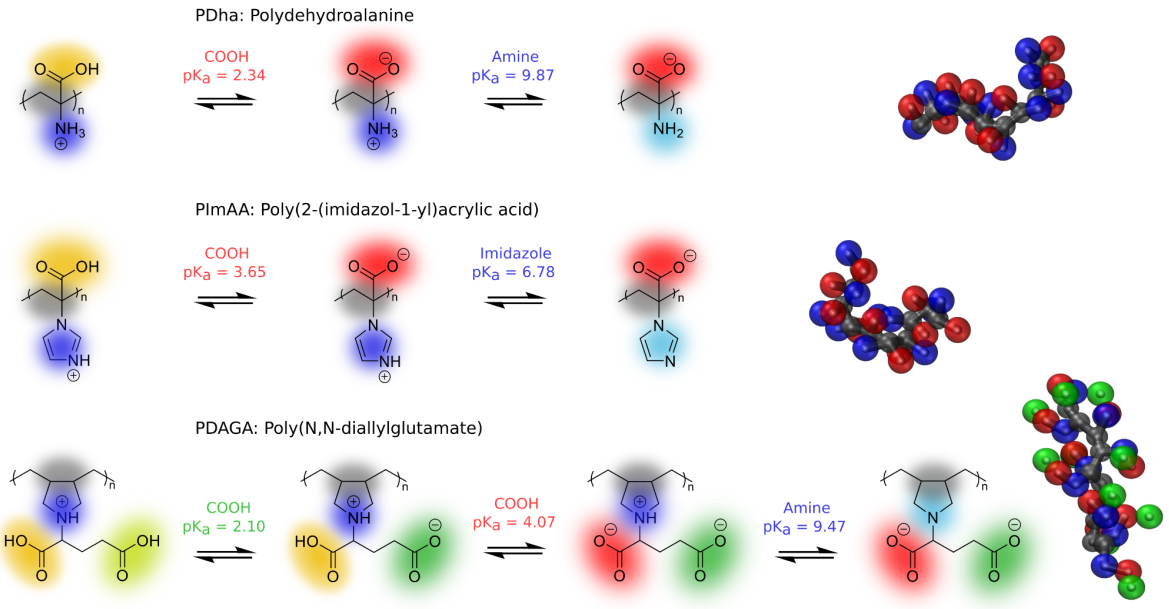

Figure 1: Overview of the investigated polyzwitterions: poly(*N,N*-diallylglutamate) (PDAGA), polydehydroalanine (PDha) and poly(2-(imidazol-1-yl)acrylic acid) (PImAA). The chemical structures on the left show the different ionization states. The simulation snapshot next to each chemical structure represents the coarse-grained model that we used for the corresponding polyzwitterion. Colour code: grey = backbone groups; red, green = acidic groups; blue = basic groups.

Results and discussion

The key characteristics of the polyzwitterions

Three polymers were synthesized as model cases to study the ionization of polyzwitterions, following the procedures summarized in Ref.[22]: poly(N,N-diallylglutamate) (PDAGA), polydehydroalanine (PDha) and poly(2-(imidazol-1-yl)acrylic acid) (PImAA). A brief description of their synthesis is given in the Materials and methods section.

The chemical structure of the polyzwitterions was confirmed by ^{1}H-NMR (Table S2). The molecular weight of the polyzwitterions was characterized by size-exclusion chromatography (SEC) measurements, which is reported in Tab. 1. PDAGA and PDha are soluble at high pH but precipitate when the pH is lowered. PDAGA showed a miscibility gap between pH 3.0 and 1.9. PDha precipitated at pH values below 5.5 and, in contrast to PDAGA, it did not solve again when the pH was further lowered.

Table 1: Molecular characteristics of polyzwitterions determined by size-exclusion chromatography (SEC) measurements, namely: number average molecular weight $\bar{M}_n$, mass average molecular weight $\bar{M}_w$, dispersity *Đ*, number-average degree of polymerization N_m.

Polyzwitterion	$\bar{M}_n$ **/ g mol^{-1}**	$\bar{M}_w$ **/ g mol^{-1}**	***Đ***	N_m[c]
PDAGA	2,100[a]	8,100[a]	3.8[a]	9
PDha	13,700[b]	27,300[b]	2.0[b]	157
PImAA	2,700[a]	3,800[a]	1.4[a]	20

a) Determined by SEC using 0,1 M Na_2HPO_4/0,05% NaN_3 pH 9 as eluent and calibrated against PAA standards;
b) Determined by SEC using DMAc/LiCl SEC as eluent and calibrated against PMMA standards.
c) Calculated from $\bar{M}_n$

Due to the presence of both cationic and anionic groups on each monomeric unit of polyzwitterions, we expect their ionization to be influenced by a complex interplay between electrostatic attraction between oppositely charged groups and repulsion between like-charged groups. To demonstrate the effects of this interplay, we computed the net charge on the zwitterions from molecular simulations and compared it with the ideal value predicted by the Henderson-Hasselbalch equation (Eq. 1). Fig.2 shows the results of these predictions, using PDAGA, PDha and PImAA as model polyzwitterions. In general, we observe that electrostatic interactions decrease the absolute value of the average charge per monomer z_m as compared to the ideal curve. Such deviations are often characterized by using effective pK_a-values (pK_a^{eff}), defined as the pH value at which the respective acid or base group is half-ionized. Nevertheless, a description using the effective pKa values does not fully account for the observed deviations because they not only shift the curves but also change their shape. To fully describe the effect, it is necessary to investigate the degree of ionization of each group, α, as a function of pH.

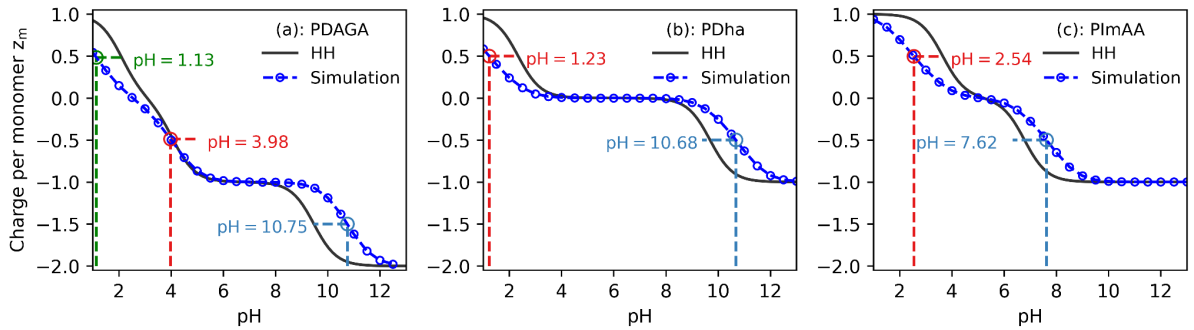

Figure 2: Average net charge per monomer z_m as a function of pH for PDAGA (a), PDha (b) and PImAA (c). Data points are from the simulations whereas the continuous lines follow the ideal prediction given by the Henderson-Hasselbalch (HH) equation (Eqs. 1 and 3). Dashed vertical lines mark the effective pKa values estimated from these curves.

Fig.3 shows the degrees of ionization of individual acid and base groups on the three investigated polyzwitterions: PDAGA, PDha and PImAA. Based on these curves, we observe that in general the ionization of each acid and base group is increased, as compared to the ideal curve, obtained from the Henderson-Hasselbalch equation. Alternatively, this difference can be viewed as a shift of the curve along the pH axis, which is often quantified using the effective acidity constant, pK_a^{eff}. The curves in Fig.3 indicate that pK_a^{eff} of the acidic groups is lower than their bare pK_a whereas pK_a^{eff} of the basic groups is greater than their bare pK_a. Furthermore, the simulated curves in Fig.3 are not only shifted with respect to the ideal curves but they also have different slopes, which cannot be described by using pK_a^{eff} as the only parameter. These observations are consistent with previous simulation studies on peptides[26,27] and weak ampholytes,[51,52] where it has been shown that this is caused by electrostatic attraction to the oppositely charged groups nearby. Because the pK_a values of these acid and base groups differ by more than 3 units, the response of each of them to changes in the pH is characterized by a clearly distinguished inflection point on the dependence of the net charge on the pH (*cf.* Fig.2).

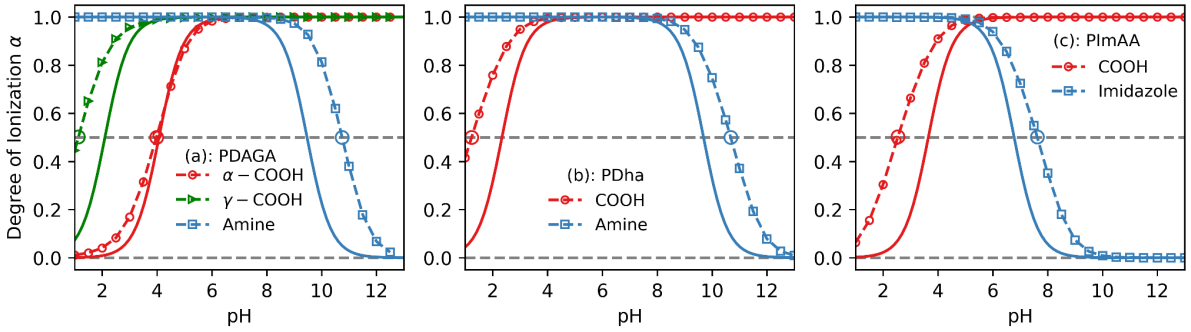

Figure 3: Degree of ionization α of each ionizable group in the monomeric units of PDAGA, PDha and PImAA as a function of pH (see legend in each panel). Data points represent predictions from the simulations whereas the continuous lines follow the corresponding ideal prediction given by the Henderson-Hasselbalch (HH) equation (Eq. 1). Dashed curves connecting the simulation data points are added as guides to the eye. Horizontal dashed lines mark the values of $\alpha = 0.0,\ 0.5,\ 1.0$.

Interpreting the titration curve of polyzwitterions

Similar to the interpretation of Fig.3, the inflection points in experimentally determined titration curves are also commonly used to identify the effective pK_a values of the titrated sample (analyte). In commercial instruments, this is done using the equivalence point recognition criterion (ERC), computed as the first derivative of the titration curve, *i.e.* first derivative of the dependence of the pH on the added volume of the reagent. In Fig.4 (top panels), we present such potentiometric titration curves, including the ERC, measured for the polyzwitterions investigated here. The pK_a^{eff} values were obtained from the ERC, following the procedure outlined in Ref.[33], as detailed in ESI, section S6. Table 2 shows that these pK_a^{eff} values often disagree with those predicted from our simulations (*cf.* Fig.2). Furthermore, the determination based on ERC indicates two pK_a^{eff} values for PDAGA and three pK_a^{eff} values for PDha although PDAGA has three ionizable groups and PDha has only two. The value $pK_a^{eff} = 6.3$ is very far from the bare pK_a values of its both ionizable groups. Because the ionization of PDha should not change close to the neutral pH, we anticipate that this pK_a^{eff} value simply reflects the steep change of the pH as HCl is being added to NaOH in the presence of an indifferent polyzwitterion. This observation suggests that determination of the pK_a^{eff} using the ERC might not be reliable.

In the bottom panels of Fig.4, we present an alternative approach to determine the pK_a^{eff} values from potentiometric titrations, using the inflection points of the net charge on the analyte as a function of pH, similar to how we did it in Fig.2. These dependencies have been calculated from the potentiometric titration curves using Eq.2, as described in full detail in the Methods section. By comparing the pK_a^{eff} values from the ERC, marked in the bottom

panels of Fig.4, we clearly see that they do not correspond to the inflection points of the net charge as a function of pH. On the contrary, we observe that the net charge as a function of pH reasonably well corresponds to the theoretical predictions for PDAGA and PDha, whereas it does not correspond with the predictions for PImAA. This confirms the notion that ERC cannot be reliably used to determine pK_a^{eff} of our samples.

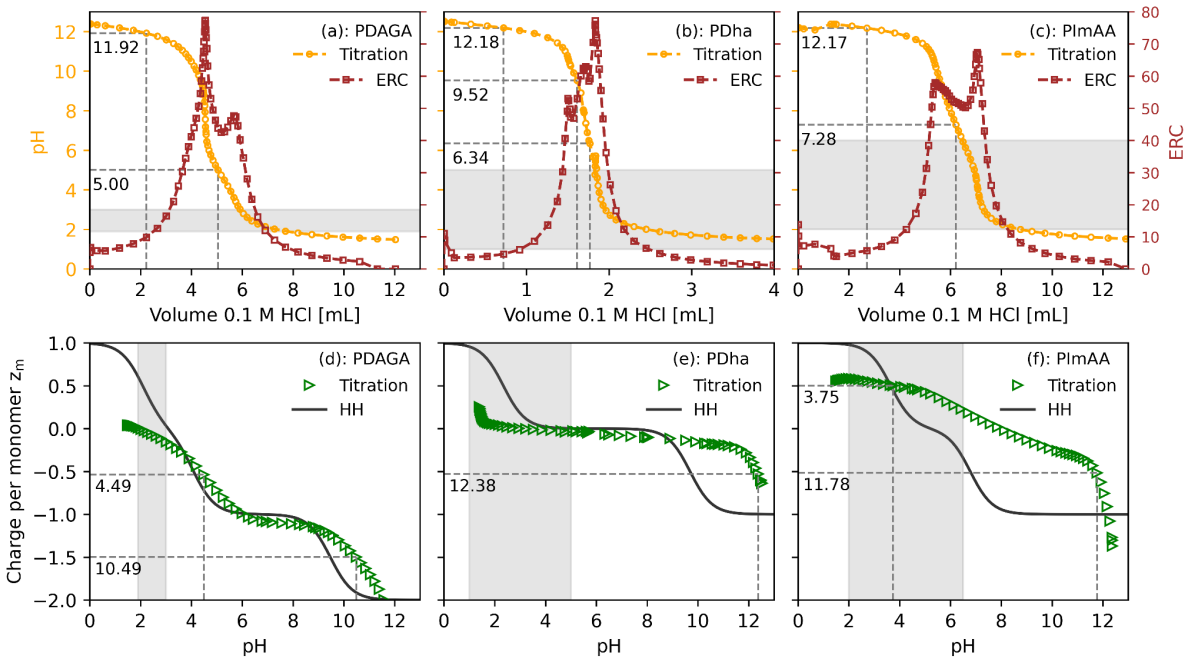

Figure 4: Top panels: potentiometric titration (orange markers) of the polyzwitterions with HCl (concentration 0.1 M). Its first derivative (brown markers) is used as the equivalence point recognition criterion (ERC). The points of half-equivalence, corresponding to the estimated effective pK_a values, are indicated using the dashed lines. Bottom panels: average charge per monomer z_m of the polyzwitterions calculated from their corresponding titration curves using Eq. 2. The dashed lines in bottom panels mark the effective pK_a values, estimated from the net charge corresponding to half-ionization of the respective groups. The solid lines follow the corresponding ideal prediction given by the Henderson-Hasselbalch (HH) equation (Eq. 1). The gray-shaded areas highlight the pH regions where we observed precipitation of the polyzwiterions.

To obtain an independent picture of the net charge on the herein used polyzwitterions as a function of pH, we measured their zeta potential ζ_p, presented in Fig.5. Unfortunately, reproducible data could only be obtained for PDAGA and PDha but not in case of PImAA. We observe that the measured ζ_p as a function of the pH qualitatively resembles the net

charge as a function of pH, shown in Fig.2 and Fig.4. In particular, the pH range in which the zeta potential steeply changes as a function of pH in Fig.5 is well matched by the steep change of the net charge in Figs.2 and 4. However, computing the net charge from the zeta potential is not straightforward because this quantity is proportional to the effective charge on the surface rather than to the net charge of the colloidal object.[23–25,27,53,54] In the case of PDAGA, we observe that the isoelectric point determined from the zeta potential (pI ~ 2.5) matches the one determined from potentiometric titrations (pI ~ 2.0, see Fig.4d) and predicted from the theory (pI ~ 2.5, see Fig.2a). In contrast, the zeta potential of PDha suggests that it should be negatively charged in a broad pH range (ranging from 4 to 11) whereas the potentiometric titrations (Fig.4e) and also the theoretical predictions (Fig.2b) suggest that it should be neutral in that pH range. Indeed, it is not a unique observation that a neutral polymer has a negative zeta potential. A similar effect has been observed for poly(ethylene oxide), e.g. as corona of micellar nanostructures, although also here no quantitative explanation has been found so far.[55,56] Therefore, the values of the zeta potential should not be taken literally. Instead, one should compare the overall trend in the zeta potential with the net charge determined using other methods.

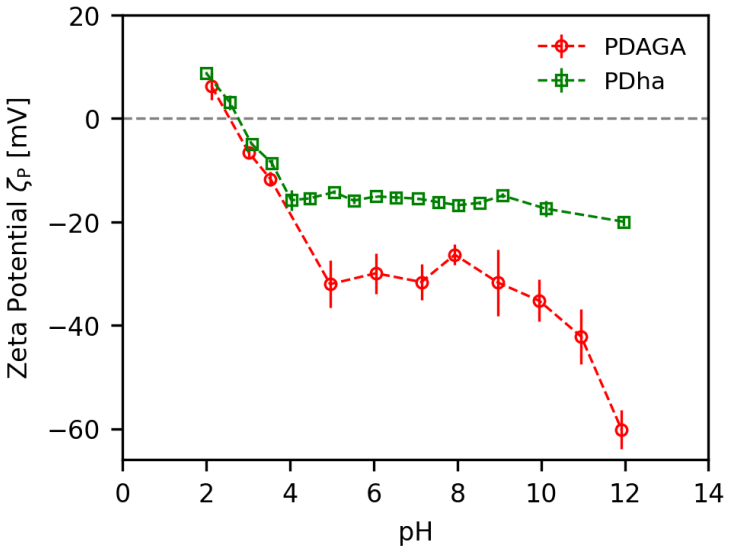

Figure 5: Zeta potential ζ_p of PDAGA (red circles) and PDha (green squares) as a function of pH. Dashed curves connecting the data points serve as a guide to the eye.

In Fig.6 we compare the three approaches (simulation, potentiometric titration and the zeta potential) of obtaining the net charge per monomer on the studied zwitterions in order to assess their reliability. To enable this comparison within a single figure, it was necessary to shift and scale the zeta potential. In the first step, we added constant values to shift the curve such that they matched the isoelectric point determined by the potentiometric titrations. This shift was practically negligible in case of PDAGA, however, it was significant in case of PDha, as discussed in the previous paragraph. In the second step, we multiplied the shifted zeta potential by an arbitrary constant such that it approximately fits on the same scale as the other data sets. After this transformation we were able to compare all three approaches within a single plot.

Fig.6a shows that in the case of PDAGA all three approaches yield consistent deviations from the ideal curve. In case of PDha (Fig.6b), the three approaches yield similar trends, namely a weakly positive charge at very acidic conditions, pH ~ 2, a constant net charge close to zero in a broad pH range, 2 < pH < 11, and a negative charge at very basic conditions, pH > 11. However, the titrations suggest that PDha attains a positive charge only

at a much lower pH than predicted by the simulations. Similarly, the titrations suggest that PDha attains a negative charge at a much higher pH than predicted by the simulations. In Fig.S4 we demonstrate that this difference can be easily avoided by using different bare pK_a values as the inputs of the simulation. It should be kept in mind that the original pK_a values used in our simulations were only based on an educated guess, using analogy with molecules of a similar chemical structure. Therefore, similar values within a reasonable range are also plausible and there is no strong reason to insist on the values determined by our educated guess. This uncertainty is clearly a weak point of any simulation which requires the bare pK_a values, as discussed also in our previous study on short peptides.[27] Finally, in Fig.6c we observe a strong disagreement between the simulation results and potentiometric titration of PImAA. Unlike PDha, the curves for PImAA differ qualitatively and this disagreement could not be avoided by choosing different bare pK_a values as simulation inputs. We may speculate that the imidazole group of PImAA exhibit some kind of hydrophobic attraction or hydrogen bonding, however, we do not have sufficient evidence to conclude about the molecular origin of the disagreement. Unfortunately, the measurements of zeta potential of PImAA did not yield reproducible values, preventing a comparison with the third available method. Nevertheless, it is clear from the above comparison that there are additional specific interactions in PImAA, other than electrostatics, which determine its peculiar response to pH.

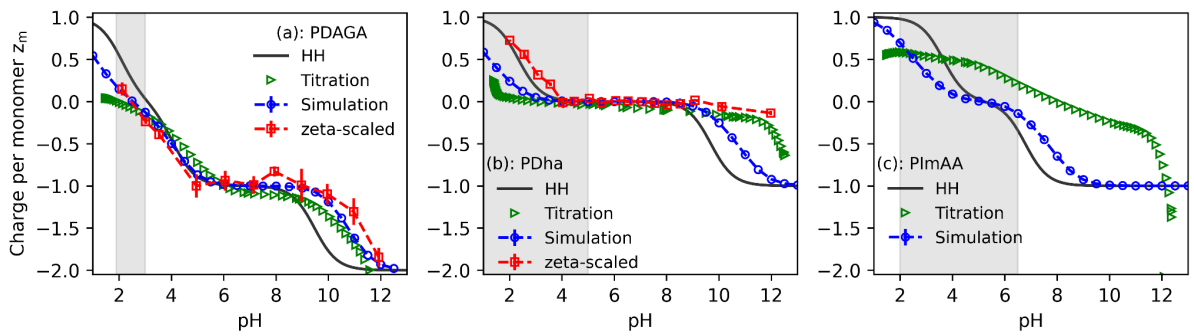

Figure 6: Net charge per monomeric unit z_m of PDAGA (a), PDha (b) and PImAA (c) as a function of pH obtained from our simulations (circles), potentiometric titration (triangles). The zeta potential (squares) of each polyzwitterion was shifted by an arbitrary constant to match the isoelectric point from potentiometric titrations and then scaled by an arbitrary constant. Continuous lines follow the ideal prediction given by the Henderson-Hasselbalch (HH) equation (Eqs. 1-2). Dashed lines are added to guide the eye and follow the data points.

Thus, by comparing the three approaches to determining the net charge of the studied polyampholytes, we can conclude that our determination of the net charge was quantitatively reliable in the case of PDAGA, qualitatively reliable in the case of PDha and unreliable in the case of PImAA. These results are summarized in Table 2. The comparison with effective pKa values determined from half-equivalence points based on the ERC determined as the first derivative of the titration curve is tricky. Table 2 demonstrates that in many cases these values are consistent with the other methods, as well as with the expectations based on simple chemical intuition. On the other hand, some values obtained from the ERC ($pK_a^{eff} = 6.3$ and $pK_a^{eff} = 12.2$ for PDha and $pK_a^{eff} = 12$ for PImAA) are most likely artifacts of the method because these values were not observed by any other of the employed methods, they are not compatible with simple chemical intuition, and in two cases there is no ionizable acid or base group to which these pKa values could be assigned.

Table 2: Effective pKa values determined using different methods, compared to the bare pKa of the monomer. Values marked with an asterisk are likely unphysical artifacts of the data processing.

Polymer	bare pKa (monomer)	simulation	zeta potential (estimated)	titration net charge	titration half-equivalence
PDAGA pKa 1	2.10	1.13	N/A	N/A	N/A
PDAGA pKa 2	4.07	3.98	3.5	4.49	5.0
PDAGA pKa 3	9.47	10.75	11.5	10.49	11.9
PDha pKa 1	2.34	1.23	3	N/A	6.3*
PDha pKa 2	9.87	10.68	N/A	N/A	9.5
PDha pKa 3	N/A	N/A	N/A	12.38	12.2*
PimAA pKa 1	3.65	2.54	N/A	3.75	< 2
PimAA pKa 2	6.78	7.62	N/A	N/A	7.3
PimAA pKa 3	N/A	N/A	N/A	11.78	12.2*

Conclusions

We combined molecular simulations with several experimental methods to investigate the ionization response of various polyzwitterions to changes in the pH. Specifically, we used poly(*N,N*-diallylglutamate) (PDAGA) with two weakly acidic groups and one weakly basic group per monomer, polydehydroalanine (PDha) and poly(2-(imidazol-1-yl)acrylic acid) (PImAA), both with one acidic and one basic group per monomer. First, we used molecular simulations to determine the net charge per monomer and the ionization states of individual acidic and basic groups as a function of pH. From the simulations we observed that the electrostatic interactions with oppositely charged groups increase the ionization states. Therefore, the effective pK_a values of the acidic groups were lower whereas the effective pK_a

values of the basic groups were higher than their respective bare pK_a values. Ultimately, these shifts resulted in reducing the net charge of the polymer, making it closer to neutral than in the ideal case without electrostatic interactions. To complement the theoretical predictions, we performed potentiometric titrations of all studied polyzwitterions. We observed that the effective pK_a values, determined from the equivalence point recognition criterion (ERC) were often inconsistent with those predicted from the simulation. In some cases, the ERC determination yielded a different number of pK_a values than the number of different titratable groups and the determined effective pK_a values were not even close to the bare pK_a values of the monomers. However, when we calculated the net charge per monomer from the potentiometric titration curves, the obtained results were consistent with the simulations in case of PDAGA and PDha. Additionally, we measured the zeta potential as a function of pH, which also yielded trends consistent with the simulations and titrations of PDAGA and PDha. Minor quantitative differences between the simulations and experiments could be explained by the uncertainty in choosing the bare pK_a values as inputs of the simulation. On the contrary, in case of PImAA our titrations yielded the net charge as a function of pH which was very different from the simulations and from the ideal trend based on the expected bare pK_a values. These differences could not be explained by the uncertainty in choosing the bare pK_a values. Therefore, we attributed them to some specific interactions in PImAA, such as hydrogen bonding, which could not be captured by the simplified molecular model.

Ultimately, by analyzing the ionization response of three model polyzwitterions to changes in the pH, we have shown that molecular simulations can predict and explain the origin of the differences between the effective and bare pK_a values of individual titratable groups. Furthermore, we have shown that it is not possible to obtain these effective pK_a values directly from the ERC, however, they can be reliably obtained by calculating the net charge per monomer from the potentiometric titration curves. This determination can be further

confirmed by the trends in the zeta potential as a function of pH, however, a quantitative parameter-free comparison with the zeta potential is not possible because zeta potential depends on the effective surface charge rather than the bare charge. The approach we propose works reliably for polyzwitterions in which the ionization response is dominated by electrostatic interactions, such as PDAGA or PDha, however, it fails if other specific interactions contribute significantly, such as in the case of PImAA. Nevertheless, the herein presented approach allows for an improved understanding of charge and solution characteristics in weak polyzwitterions and, with that, also in an improved prediction and description of their behavior at interfaces or interaction with other charged molecules, *e.g.*, in „catch and release“ approaches or as coatings of nanomaterials.

Supporting Information

Additional technical details about the computer simulations, ^{1}H-NMR characterization of the three polyzwitterions of study, additional plots of computer simulations of polyzwiterrions with different chain lengths, additional plots of computer simulations done with different input bare pK_a values, additional plots of control potentiometric titrations done with blank samples.

Acknowledgements

R.L., A.M., P.M.B., M.Š. and P.K. acknowledge financial support from the Czech Science Foundation, project No. 19-10429S. The authors are further grateful for financial support through the Deutsche Forschungsgemeinschaft (DFG, SCHA1640/12-1: F.H.S. and P.B., and project TP02 within FOR2811 – project no. 423435478, F.H.S. and P.M.). P.M.B. also acknowledges the financial support of the grant Margarita Salas from the University of Barcelona (funded by the Spanish Ministry of Universities and the European Union).

Computational resources were provided by the project "e-Infrastruktura CZ" (e-INFRA CZ LM2018140) supported by the Ministry of Education, Youth and Sports of the Czech Republic.

Electronic supporting information (ESI) is available.

Bibliography

(1) Sin, M.-C.; Chen, S.-H.; Chang, Y. Hemocompatibility of Zwitterionic Interfaces and Membranes. *Polym. J.* **2014**, *46* (8), 436–443. https://doi.org/10.1038/pj.2014.46.

(2) Zhang, Y.; Liu, Y.; Ren, B.; Zhang, D.; Xie, S.; Chang, Y.; Yang, J.; Wu, J.; Xu, L.; Zheng, J. Fundamentals and Applications of Zwitterionic Antifouling Polymers. *J. Phys.*

Appl. Phys. **2019**, *52* (40), 403001. https://doi.org/10.1088/1361-6463/ab2cbc.
(3) Hess, M.; Jones, R. G.; Kahovec, J.; Kitayama, T.; Kratochvíl, P.; Kubisa, P.; Mormann, W.; Stepto, R. F. T.; Tabak, D.; Vohlídal, J.; Wilks, E. S. Terminology of Polymers Containing Ionizable or Ionic Groups and of Polymers Containing Ions (IUPAC Recommendations 2006). *Pure Appl. Chem.* **2006**, *78* (11), 2067–2074. https://doi.org/10.1351/pac200678112067.
(4) Paschke, S.; Lienkamp, K. Polyzwitterions: From Surface Properties and Bioactivity Profiles to Biomedical Applications. *ACS Appl. Polym. Mater.* **2020**, *2* (2), 129–151. https://doi.org/10.1021/acsapm.9b00897.
(5) Kalasin, S.; Letteri, R. A.; Emrick, T.; Santore, M. M. Adsorbed Polyzwitterion Copolymer Layers Designed for Protein Repellency and Interfacial Retention. *Langmuir* **2017**, *33* (47), 13708–13717. https://doi.org/10.1021/acs.langmuir.7b03391.
(6) Ishihara, K.; Takayama, R.; Nakabayashi, N.; Fukumoto, K.; Aoki, J. Improvement of Blood Compatibility on Cellulose Dialysis Membrane2. Blood Compatibility of Phospholipid Polymer Grafted Cellulose Membrane. *Biomaterials* **1992**, *13* (4), 235–239. https://doi.org/10.1016/0142-9612(92)90190-Y.
(7) Kumar, R.; Fredrickson, G. H. Theory of Polyzwitterion Conformations. *J. Chem. Phys.* **2009**, *131* (10), 104901. https://doi.org/10.1063/1.3216107.
(8) Higaki, Y.; Nishida, J.; Takenaka, A.; Yoshimatsu, R.; Kobayashi, M.; Takahara, A. Versatile Inhibition of Marine Organism Settlement by Zwitterionic Polymer Brushes. *Polym. J.* **2015**, *47* (12), 811–818. https://doi.org/10.1038/pj.2015.77.
(9) García, K. P.; Zarschler, K.; Barbaro, L.; Barreto, J. A.; O'Malley, W.; Spiccia, L.; Stephan, H.; Graham, B. Zwitterionic-Coated "Stealth" Nanoparticles for Biomedical Applications: Recent Advances in Countering Biomolecular Corona Formation and Uptake by the Mononuclear Phagocyte System. *Small* **2014**, *10* (13), 2516–2529. https://doi.org/10.1002/smll.201303540.
(10) Shimizu T.; Ishima Y.; Ishida T. Induction of Anti-PEG Immune Responses by PEGylation of Proteins. *YAKUGAKU ZASSHI* **2020**, *140* (2), 163–169. https://doi.org/10.1248/yakushi.19-00187-5.
(11) Schönemann, E.; Laschewsky, A.; Wischerhoff, E.; Koc, J.; Rosenhahn, A. Surface Modification by Polyzwitterions of the Sulfabetaine-Type, and Their Resistance to Biofouling. *Polymers* **2019**, *11* (6), 1014. https://doi.org/10.3390/polym11061014.
(12) Debayle, M.; Balloul, E.; Dembele, F.; Xu, X.; Hanafi, M.; Ribot, F.; Monzel, C.; Coppey, M.; Fragola, A.; Dahan, M.; Pons, T.; Lequeux, N. Zwitterionic Polymer Ligands: An Ideal Surface Coating to Totally Suppress Protein-Nanoparticle Corona Formation? *Biomaterials* **2019**, *219*, 119357. https://doi.org/10.1016/j.biomaterials.2019.119357.
(13) Laschewsky, A. Structures and Synthesis of Zwitterionic Polymers. *Polymers* **2014**, *6* (5), 1544–1601. https://doi.org/10.3390/polym6051544.
(14) Lee, E. S.; Oh, K. T.; Kim, D.; Youn, Y. S.; Bae, Y. H. Tumor PH-Responsive Flower-like Micelles of Poly(l-Lactic Acid)-b-Poly(Ethylene Glycol)-b-Poly(l-Histidine). *J. Controlled Release* **2007**, *123* (1), 19–26. https://doi.org/10.1016/j.jconrel.2007.08.006.
(15) Hrubý, M.; Filippov, S. K.; Štěpánek, P. Smart Polymers in Drug Delivery Systems on Crossroads: Which Way Deserves Following? *Eur. Polym. J.* **2015**, *65*, 82–97. https://doi.org/10.1016/j.eurpolymj.2015.01.016.
(16) Yaagoob, I. Y.; Al-Muallem, H. A.; Ali, S. A. Synthesis and Application of Polyzwitterionic and Polyampholytic Maleic Acid-Alt-(Diallylamino)Propylphosphonates. *RSC Adv.* **2017**, *7* (50), 31641–31653. https://doi.org/10.1039/C7RA04418F.
(17) Kudaibergenov, S. E.; Nuraje, N. Intra- and Interpolyelectrolyte Complexes of Polyampholytes. *Polymers* **2018**, *10*, 1146–1180. https://doi.org/10.3390/polym10101146.
(18) Choi, J.; Rubner, M. F. Influence of the Degree of Ionization on Weak Polyelectrolyte

Multilayer Assembly. *Macromolecules* **2005**, *38* (1), 116–124. https://doi.org/10.1021/ma048596o.
(19) Günther, U.; Sigolaeva, L. V.; Pergushov, D. V.; Schacher, F. H. Polyelectrolytes with Tunable Charge Based on Polydehydroalanine: Synthesis and Solution Properties. *Macromol. Chem. Phys.* **2013**, *214* (19), 2202–2212. https://doi.org/10.1002/macp.201300324.
(20) von der Lühe, M.; Günther, U.; Weidner, A.; Gräfe, C.; Clement, J. H.; Dutz, S.; Schacher, F. H. SPION@polydehydroalanine Hybrid Particles. *RSC Adv.* **2015**, *5* (40), 31920–31929. https://doi.org/10.1039/C5RA01737H.
(21) Biehl, P.; von der Lühe, M.; Dutz, S.; Schacher, F. Synthesis, Characterization, and Applications of Magnetic Nanoparticles Featuring Polyzwitterionic Coatings. *Polymers* **2018**, *10* (1), 91. https://doi.org/10.3390/polym10010091.
(22) Biehl, P.; Wiemuth, P.; Lopez, J. G.; Barth, M.-C.; Weidner, A.; Dutz, S.; Peneva, K.; Schacher, F. H. Weak Polyampholytes at the Interface of Magnetic Nanocarriers: A Facile Catch-and-Release Platform for Dyes. *Langmuir* **2020**, *36* (22), 6095–6105. https://doi.org/10.1021/acs.langmuir.0c00455.
(23) Griffiths, P. C.; Paul, A.; Stilbs, P.; Petterson, E. Charge on Poly(Ethylene Imine): Comparing Electrophoretic NMR Measurements and PH Titrations. *Macromolecules* **2005**, *38* (8), 3539–3542. https://doi.org/10.1021/ma0478409.
(24) Böhme, U.; Scheler, U. Counterion Condensation and Effective Charge of Poly(Styrenesulfonate). *Adv. Colloid Interface Sci.* **2010**, *158* (1–2), 63–67. https://doi.org/10.1016/j.cis.2010.02.010.
(25) Huber, K.; Scheler, U. New Experiments for the Quantification of Counterion Condensation. *Curr. Opin. Colloid Interface Sci.* **2012**, *17* (2), 64–73. https://doi.org/10.1016/j.cocis.2012.01.005.
(26) Lunkad, R.; Murmiliuk, A.; Tošner, Z.; Štěpánek, M.; Košovan, P. Role of PKA in Charge Regulation and Conformation of Various Peptide Sequences. *Polymers* **2021**, *13* (2), 214. https://doi.org/10.3390/polym13020214.
(27) Lunkad, R.; Murmiliuk, A.; Hebbeker, P.; Boublík, M.; Tošner, Z.; Štěpánek, M.; Košovan, P. Quantitative Prediction of Charge Regulation in Oligopeptides. *Mol. Syst. Des. Eng.* **2021**, *6* (2), 122–131. https://doi.org/10.1039/D0ME00147C.
(28) Hass, M. A. S.; Mulder, F. A. A. Contemporary NMR Studies of Protein Electrostatics. *Annu. Rev. Biophys.* **2015**, *44* (1), 53–75. https://doi.org/10.1146/annurev-biophys-083012-130351.
(29) Müller, M.; Wirth, L.; Urban, B. Determination of the Carboxyl Dissociation Degree and PK_a Value of Mono and Polyacid Solutions by FTIR Titration. *Macromol. Chem. Phys.* **2021**, *222* (4), 2000334. https://doi.org/10.1002/macp.202000334.
(30) Wang, J.; Xie, M.; Wang, H.; Xu, S. Solvent Extraction and Separation of Heavy Rare Earths from Chloride Media Using Nonsymmetric (2,3-Dimethylbutyl)(2,4,4′-Trimethylpentyl)Phosphinic Acid. *Hydrometallurgy* **2017**, *167*, 39–47. https://doi.org/10.1016/j.hydromet.2016.10.020.
(31) Kraft, A. The Determination of the PKa of Multiprotic, Weak Acids W by Analyzing Potentiometric Acid–Base Titration Data with Difference Plots. *J. Chem. Educ.* **2003**, *80* (5), 554–559.
(32) Subirats, X.; Fuguet, E.; Rosés, M.; Bosch, E.; Ràfols, C. Methods for PKa Determination (I): Potentiometry, Spectrophotometry, and Capillary Electrophoresis. In *Reference Module in Chemistry, Molecular Sciences and Chemical Engineering*; Elsevier, 2015; p B9780124095472116000. https://doi.org/10.1016/B978-0-12-409547-2.11559-8.
(33) Lazzari, F.; Manfredi, A.; Alongi, J.; Marinotto, D.; Ferruti, P.; Ranucci, E. D-, l- and d,l-Tryptophan-Based Polyamidoamino Acids: PH-Dependent Structuring and

Fluorescent Properties. *Polymers* **2019**, *11* (3), 543. https://doi.org/10.3390/polym11030543.
(34) Kalka, H. Polyprotic Acids and Beyond—An Algebraic Approach. *Chemistry* **2021**, *3* (2), 454–508. https://doi.org/10.3390/chemistry3020034.
(35) Colombani, O.; Lejeune, E.; Charbonneau, C.; Chassenieux, C.; Nicolai, T. Ionization Of Amphiphilic Acidic Block Copolymers. *J. Phys. Chem. B* **2012**, *116* (25), 7560–7565. https://doi.org/10.1021/jp3012377.
(36) Shedge, A.; Colombani, O.; Nicolai, T.; Chassenieux, C. Charge Dependent Dynamics of Transient Networks and Hydrogels Formed by Self-Assembled PH-Sensitive Triblock Copolyelectrolytes. *Macromolecules* **2014**, *47* (7), 2439–2444. https://doi.org/10.1021/ma500318m.
(37) Farias-Mancilla, B.; Zhang, J.; Kulai, I.; Destarac, M.; Schubert, U. S.; Guerrero-Sanchez, C.; Harrisson, S.; Colombani, O. Gradient and Asymmetric Copolymers: The Role of the Copolymer Composition Profile in the Ionization of Weak Polyelectrolytes. *Polym. Chem.* **2020**, *11* (47), 7562–7570. https://doi.org/10.1039/D0PY01059F.
(38) Jamiu, Z. A.; Al-Muallem, H. A.; Ali, S. A. A Glutamic Acid-Based Polymer Keeping Intact the Integrity of All the Three Original Functionalities of the Amino Acid. *Des. Monomers Polym.* **2016**, *19* (2), 128–137. https://doi.org/10.1080/15685551.2015.1124320.
(39) Rössel, C.; Billing, M.; Görls, H.; Festag, G.; Grube, M.; Bellstedt, P.; Nischang, I.; Schacher, F. H. Synthesis and Modification of Poly(Ethyl 2-(Imidazol-1-Yl)Acrylate) (PEImA). *Polymer* **2017**, *127*, 182–191. https://doi.org/10.1016/j.polymer.2017.08.058.
(40) Landsgesell, J.; Nová, L.; Rud, O.; Uhlík, F.; Sean, D.; Hebbeker, P.; Holm, C.; Košovan, P. Simulations of Ionization Equilibria in Weak Polyelectrolyte Solutions and Gels. *Soft Matter* **2019**, *15* (6), 1155–1185. https://doi.org/10.1039/C8SM02085J.
(41) Lunkad, R.; Barroso da Silva, F. L.; Košovan, P. Both Charge-Regulation and Charge-Patch Distribution Can Drive Adsorption on the Wrong Side of the Isoelectric Point. *J. Am. Chem. Soc.* **2022**, *144* (4), 1813–1825. https://doi.org/10.1021/jacs.1c11676.
(42) Nová, L.; Uhlík, F.; Košovan, P. Local PH and Effective PK_A of Weak Polyelectrolytes – Insights from Computer Simulations. *Phys. Chem. Chem. Phys.* **2017**, *19* (22), 14376–14387. https://doi.org/10.1039/C7CP00265C.
(43) Murmiliuk, A.; Košovan, P.; Janata, M.; Procházka, K.; Uhlík, F.; Štěpánek, M. Local PH and Effective p *K* of a Polyelectrolyte Chain: Two Names for One Quantity? *ACS Macro Lett.* **2018**, *7* (10), 1243–1247. https://doi.org/10.1021/acsmacrolett.8b00484.
(44) Blanco, P. M.; Madurga, S.; Mas, F.; Garcés, J. L. Effect of Charge Regulation and Conformational Equilibria in the Stretching Properties of Weak Polyelectrolytes. *Macromolecules* **2019**, *52* (21), 8017–8031. https://doi.org/10.1021/acs.macromol.9b01160.
(45) Stornes, M.; Blanco, P. M.; Dias, R. S. Polyelectrolyte-Nanoparticle Mutual Charge Regulation and Its Influence on Their Complexation. *Colloids Surf. Physicochem. Eng. Asp.* **2021**, *628*, 127258. https://doi.org/10.1016/j.colsurfa.2021.127258.
(46) Staňo, R.; Nová, L.; Uhlík, F.; Košovan, P. Multivalent Counterions Accumulate in Star-like Polyelectrolytes and Collapse the Polymer in Spite of Increasing Its Ionization. *Soft Matter* **2020**, *16* (4), 1047–1055. https://doi.org/10.1039/C9SM02318F.
(47) Blanco, P. M.; Madurga, S.; Garcés, J. L.; Mas, F.; Dias, R. S. Influence of Macromolecular Crowding on the Charge Regulation of Intrinsically Disordered Proteins. *Soft Matter* **2021**, *17* (3), 655–669. https://doi.org/10.1039/D0SM01475C.
(48) Lide, D. R. *Handbook of Chemistry and Physics*, 72nd ed.; CRC press: Boca Raton, 1991.

(49) Haynes, W. M.; Lide, D. R.; Bruno, T. J. *CRC Handbook of Chemistry and Physics*; CRC press, 2016.
(50) Human Metabolome Database. Imidazoleacetic Acid.
(51) Ulrich, S.; Seijo, M.; Stoll, S. A Monte Carlo Study of Weak Polyampholytes: Stiffness and Primary Structure Influences on Titration Curves and Chain Conformations. *J. Phys. Chem. B* **2007**, *111* (29), 8459–8467. https://doi.org/10.1021/jp0688658.
(52) Ulrich, S.; Seijo, M.; Carnal, F.; Stoll, S. Formation of Complexes between Nanoparticles and Weak Polyampholyte Chains. Monte Carlo Simulations. *Macromolecules* **2011**, *44* (6), 1661–1670. https://doi.org/10.1021/ma1024895.
(53) Hill, R. J.; Saville, D. A.; Russel, W. B. Electrophoresis of Spherical Polymer-Coated Colloidal Particles. *J. Colloid Interface Sci.* **2003**, *258* (1), 56–74. https://doi.org/10.1016/S0021-9797(02)00043-7.
(54) Lobaskin, V.; Dünweg, B.; Holm, C. Electrophoretic Mobility of a Charged Colloidal Particle: A Computer Simulation Study. *J. Phys. Condens. Matter* **2004**, *16* (38), S4063–S4073. https://doi.org/10.1088/0953-8984/16/38/021.
(55) Barthel, M. J.; Rinkenauer, A. C.; Wagner, M.; Mansfeld, U.; Hoeppener, S.; Czaplewska, J. A.; Gottschaldt, M.; Träger, A.; Schacher, F. H.; Schubert, U. S. Small but Powerful: Co-Assembly of Polyether-Based Triblock Terpolymers into Sub-30 Nm Micelles and Synergistic Effects on Cellular Interactions. *Biomacromolecules* **2014**, *15* (7), 2426–2439. https://doi.org/10.1021/bm5002894.
(56) Press, A. T.; Ramoji, A.; vd Lühe, M.; Rinkenauer, A. C.; Hoff, J.; Butans, M.; Rössel, C.; Pietsch, C.; Neugebauer, U.; Schacher, F. H.; Bauer, M. Cargo–Carrier Interactions Significantly Contribute to Micellar Conformation and Biodistribution. *NPG Asia Mater.* **2017**, *9* (10), e444–e444. https://doi.org/10.1038/am.2017.161.